Magnetization of the Layer Compounds $AFe^{II}Fe^{III}(C_2O_4)_3$ (A = Organic Cation), in Low and High Magnetic Fields: Manifestation of Néel N and Q Type Ferrimagnetism in a Molecular Lattice†

Christopher J. Nuttall and Peter Day*

Davy Faraday Research Laboratory, The Royal Institution of Great Britain, 21 Albemarle Street, London W1X 4BS, U.K.

Received March 23, 1998. Revised Manuscript Received June 5, 1998

Detailed bulk magnetization and magnetic susceptibility measurements are reported for representative examples of the series of ferrimagnetic tris-oxalato-ferrate(II,III) salts with general formula $AFe^{II}Fe^{III}(C_2O_4)_3$ (A = quaternary ammonium, phosphonium, or arsonium). The compounds all crystallize in two-dimensional hexagonal honeycomb lattices, but while some show conventional low field positive magnetization at low temperature (Néel type Q), others show a large negative magnetization below a compensation temperature T_{comp} (Néel type N) under the same measurement protocol. Isothermal and temperature-dependent magnetizations are measured after zero field and field cooling. Temperature-dependent hysteresis measurements are also presented. In compounds that exhibit negative magnetization a discontinuity in the magnetization is observed at T_t ($T_{comp} < T_t < T_c$) which correlates with the onset of a giant anisotropy and is indicative of a magnetostrictive transition. In compounds that exhibit positive magnetization, hysteresis behavior and frequency-dependent ac susceptibility data indicate a glassy magnetic order at low temperatures, possibly arising from the frustration of random anisotropy domains below a characteristic blocking temperature or imbalance and disorder of Fe(II) and Fe(III).

Introduction

One of the most remarkable features of molecular-based materials is the way that the magnetic properties may be transformed by quite small and subtle variations in the molecular chemistry.[1] A striking example of this general statment is the elegant and diverse series of two-dimensional molecular-based magnetic materials formed by tris-oxalato salts containing both divalent and trivalent transition metal ions and a wide range of organic cations, principally tetraalkyl- and tetraarylphosphonium, -arsonium, and -ammonium.[2] The common formula is $AM^{II}M'^{III}(C_2O_4)_3$ (A = organic cation), and the M and M′ alternate in a hexagonal planar honeycomb lattice, bridged by the ambidentate oxalate ions.[3−5] Depending on M and M′ the near-neighbor exchange may be ferro- or antiferromagnetic, leading to bulk ferro- or ferrimagnetic behavior. We surveyed the structures and magnetic properties of a large number of $Mn^{II}Fe^{III}$ and $Fe^{II}Fe^{III}$ examples with different A and found that the magnetic ground state was extremely sensitive to small chemical variations in A.[6] In particular, we found that in the $Fe^{II}Fe^{III}$ series the low field magnetization became large and negative at low temperature for some A's, but not others.[7] Essentially, the compounds behaved as N type or Q type according to Néel's classification of ferrimagnets.[8] In the present article we present a more detailed magnetic study with a focus on one example of each order type (A = $N(n\text{-}C_4H_9)_4$ and $P(C_6H_5)_4$), in an endeavor to find the factors determining the characteristics of the two types of behavior, in particular the negative magnetization. Magnetization, susceptibility, and hysteresis data have been determined over a wide range of temperature and applied magnetic field, paying special attention to the zero field or field cooling protocols.

Experimental Section

The compounds were prepared and characterized as described in ref 5. dc magnetic measurements were performed on a MPMS7 Quantum Design SQUID magnetometer equipped with a 7 T magnet in the temperature range 2−300 K. Powder samples of ∼30 mg (∼3 × 3 × 6 mm^3) were loaded into gel caps and placed in tight fitting transparent straws, periodically

† Dedicated to the memory of Jean Rouxel, pioneer of layer materials.

(1) For numerous recent examples, see, e.g.: Kahn, O., Ed. *Magnetism a Supramolecular Function*; Kluwer Academic Publishers: Dordrecht, 1996.

(2) Tamaki, H.; Zhong, Z. J.; Matsumoto, N.; Kida, S.; Koikawa, M.; Achiwa, N.; Hashimoto, Y.; Ookawa, H. *J. Am. Chem. Soc.* **1992**, *114*, 6974−6979.

(3) Decurtins, S.; Schmalle, H. W.; Oswald, H. R.; Linden, A.; Ensling, J.; Gutlich, P.; Hauser, A. *Inorg. Chim. Acta* **1994**, 65−73.

(4) Atovymann, O. L.; Shilov, G. V.; lyubovskaya, R. N.; Zhilyaeva, E. I.; Ovaneseyan, N. S.; L., P. S.; Gusakovskaya, I. G.; G., M. Y. *JETP Lett.* **1993**, *58*, 767−768.

(5) Carling, S. G.; Mathonière, C.; Day, P.; Malik, K. M. A.; Coles, S. J.; Hursthouse, M. B. *J. Chem. Soc., Dalton Trans.* **1996**, 1839.

(6) Mathoniere, C.; Nuttall, C. J.; Carling, S. G.; Day, P. *Inorg. Chem.* **1996**, *35*, 1201−1207.

(7) Mathoniere, C. C., S. G.; Yusheng, D.; Day, P. *J. Chem. Soc., Chem. Commun.* **1994**, 1551−1552.

(8) Neel, L. *Ann. Phys. (Paris)* **1948**, *3*, 137−198.

10.1021/cm980177g CCC: $15.00
Published on Web 08/22/1998

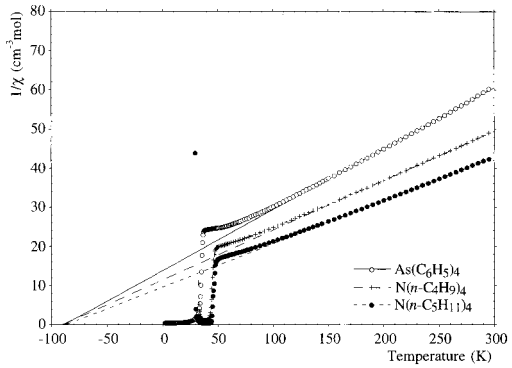

Figure 1. Inverse susceptibility vs temperature of $AFe^{II}Fe^{III}(C_2O_4)_3$ fitted to the Curie−Weiss law.

punctured with tiny holes along their length. The straws were then loaded with three compensatory empty gel caps on either side of the one containing the sample.

Low Field dc SQUID Magnetometry. Remanent fields in the magnetometer were reduced and calibrated before (and after) measurement. Large remanent fields (∼1−10 G) were reduced via the magnet reset option. Persistent remanence was calibrated by measuring samples in a paramagnetic regime, in a range of applied fields above and below (+10 G ↔ −10 G). By this means zero effective field could be accurately achieved in the magnetometer down to ±0.05 G. Remanent field creep during prolonged measurement was monitored by recalibrating remanence after completing the measurement. Low field measurements were carried out with the magnet in its oscillation field setting mode.

High Field DC SQUID Magnetometry. High field hysteresis measurements were carried out with the magnet set in the no-overshoot field setting mode, using the hysteresis option. In all high field measurements samples were rigidly held in the sample mount by pressing and placing in an inverted gel cap.

AC Magnetometry. ac susceptibility measurements were performed at the Institute of Molecular Science in Okazaki National Science Park, Japan, on a MPMS2 SQUID magnetometer fitted with an ac measurement option. Measurements were recorded between 0.01 and 1500 Hz, from 2 to 100 K. The driving field was maintained at 5 G for all measurements and zero applied dc field was rigorously maintained.

Results

Survey of Magnetic Properties. The basic magnetic characterization of all members of the series was carried out by cooling polycrystalline samples in 100 G field (100 G FC) to 2 or 5 K and measuring the magnetization at 100 G while warming to 300 K. The susceptibilities were fitted to the Curie−Weiss law from 150 to 300 K, after correcting for sample diamagnetism. Figure 1 shows the susceptibilities of the $As(C_6H_5)_4$, $N(n\text{-}C_4H_9)_4$, and $N(n\text{-}C_5H_{11})_4$ compounds. Those of other members of the series will be found in ref 6. The Curie−Weiss parameters extracted from these data will be found in Table 1.

The temperature dependence of the molar magnetizations of several of the compounds from 5 to 50 K is shown in Figure 2 and the resulting magnetic parameters in Table 1. From Figure 2, it is clear that there are two quite different kinds of temperature dependence. The magnetization of the $P(C_6H_5)_4$ and $As(C_6H_5)_4$ compounds increases abruptly below about 35 K and continues to increase monotonically, tending to saturation with $M/T \rightarrow 0$ at the lowest temperature. In striking contrast, the $N(n\text{-}C_3H_7)_4$, $N(n\text{-}C_4H_9)_4$, $N(n\text{-}C_5H_{11})_4$, $P(n\text{-}C_4H_9)_4$, and PPN compounds behave quite differently after 100 G FC. Below $T_c \sim 45$ K, the magnetization increases abruptly to reach a rounded maximum at $T_{max} \approx 40$ K ($\delta^2 M/\delta T^2$ is negative in the region 35 K < T < 42 K). It then falls rapidly and monotonically until, at about 30 K (T_{comp}), it reaches zero. At lower temperatures the magnetization becomes large and negative with respect to the applied field, tending to saturation at the lowest temperature, with $M/T \rightarrow 0$. To throw more light on this peculiar magnetic behavior, detailed magnetization measurements were made on the $N(n\text{-}C_4H_9)_4$ compound, which exhibits a negative magnetization at low temperature, and the $P(C_6H_5)_4$ compound, which has a positive magnetization.

Negative Low Temperature Magnetization. *Low Applied Fields.* The $N(n\text{-}C_4H_9)_4$ sample was cooled in fields between 0 and 100 G and the magnetization measured from 5 to 50 K in a field of 100 G. Both the ZFC and 100 G FC magnetizations increase at $T_c = 45$ K but they diverge at 43.5 K, indicating the onset of hysteresis. The ZFC magnetization reaches a maximum at 42 K and then falls, with a pronounced shoulder at 40 K, to a minimum around 35 K, after which it rises slowly toward lower temperatures. Cooling in very small fields (H < 1 G) results in negative magnetization. For example, an applied field of only 2 G during cooling gave the same negative saturation magnetization as the 100 G FC measurement (Figure 3).

The shoulder in the ZFC magnetization at 40 K was also evident as a slight discontinuity in 100-G FC magnetizations of all the compounds that showed low temperature negative magnetization. To examine this effect in more detail the $N(n\text{-}C_4H_9)_4$ compound was cooled from the paramagnetic regime to 45 K in 100 G applied field and the magnetization measured from 45 to 35 K in small temperature intervals. The resulting magnetization curve (Figure 4) has a pronounced discontinuity at 40.0 K (T_t), without significant temperature hysteresis between cooling and warming (Figure 4 inset).

To investigate the sensitivity of the low temperature magnetization to the temperature at which the field was applied, the sample was cooled successively in zero field to 45 K ($T > T_c$), 43 K ($T_t < T < T_c$), and 40 K ($T = T_t$) before further field cooling in 100 G to 5 K. Applying the field from 45 and 43 K resulted in behavior almost identical to the 100-G FC case, while field cooling from 40 K gave a magnetization curve intermediate between the FC and ZFC behavior, indicating that the sample had been cooled partially in magnetized and demagnetized states.

High Applied Field. To probe the stability of the negative magnetization state the $N(n\text{-}C_4H_9)_4$ compound was cooled in fields from 100 to 70 000 G, measuring the magnetization during warming from 5 to 50 K in an applied field of 100 G. Cooling in fields from 100 to 2000 G increased the negative saturation magnetization at 5 K, while in higher cooling fields, the saturation magnetization became progressively more positive, as shown in Figure 5. Only at the highest cooling fields (60 000−70 000 G) did the magnetization curves tend to the inverse of the 100-G FC case, with a compensation temperature at 32 K and magnetization becoming positive on decreasing temperature. Above 37 K the

Table 1. Magnetic Parameters of $AFe^{II}Fe^{III}(C_2O_4)_3$ (100-G FC)

A	T_c[a] (K)	T_{comp} (K)	C (cm^3 mol^{-1} K) (150−300 K)	θ (K) (150−300 K)	μ_{eff} ($\mu\beta$) (300 K)	M_{sat} (at T_{min}) (cm^3 G mol^{-1})
$N(n\text{-}C_3H_7)_4$	44.5	34	7.79(13)	−92.2(5.0)	6.88	−385 (2 K)
$N(n\text{-}C_4H_9)_4$	45	31.5	7.88(1)	−90.24(30)	6.87	−404 (5 K)
$N(n\text{-}C_5H_{11})_4$	46	29.5	9.05(1)	−86.92(6)	7.45	−850 (5 K)
$P(C_6H_5)_4$	34		6.71(12)	−88.4(2)	6.43	243 (2 K)
$As(C_6H_5)_4$	36		6.41(10)	−88.5(5.8)	6.27	290 (2 K)
$P(n\text{-}C_4H_9)_4$	44.5	33.5	7.761(10)	−89.9(2)	6.93	−392 (5 K)
PPN	43	30.5	7.758(10)	−88.4(2)	6.92	−235.5 (5 K)

[a] T_c chosen as the temperature of the abrupt increase in 100-G FC magnetisation.

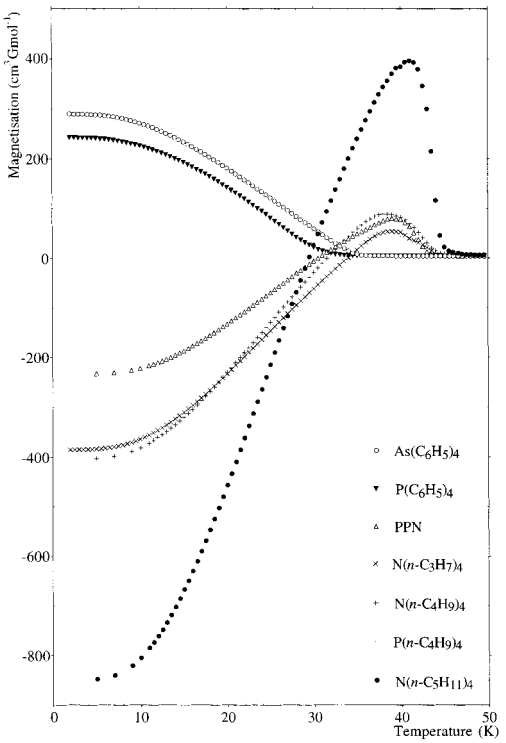

Figure 2. Temperature dependence of the magnetization of $AFe^{II}Fe^{III}(C_2O_4)_3$ after 100-G field cooling.

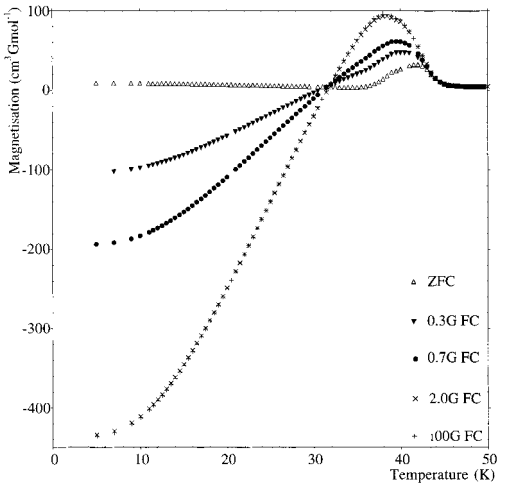

Figure 3. Temperature dependence of the ZFC and FC (0−100 G) magnetization of $N(n\text{-}C_4H_9)_4Fe^{II}Fe^{III}(C_2O_4)_3$ below 50 K.

magnetization returned to the direction of the field with a second T_{comp} = 39.5 K.

Hysteresis loops (±70 000 G) were recorded at 5 K after 100-G FC, 70 000-G FC, and ZFC. The hysteresis curve after 100-G FC (Figure 6) is asymmetrically

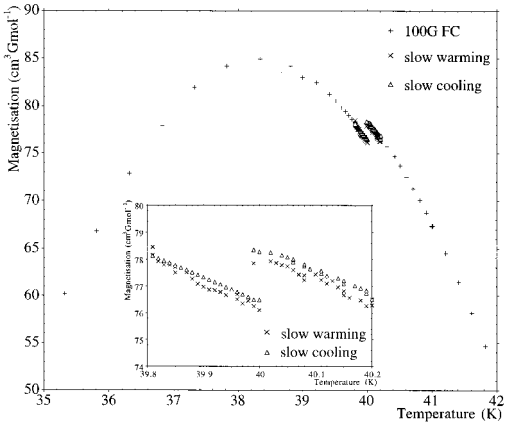

Figure 4. Magnetization of $N(n\text{-}C_4H_9)_4Fe^{II}Fe^{III}(C_2O_4)_3$ (100-G FC) showing the discontinuity at 40 K. The inset shows slow warming and slow cooling cycles.

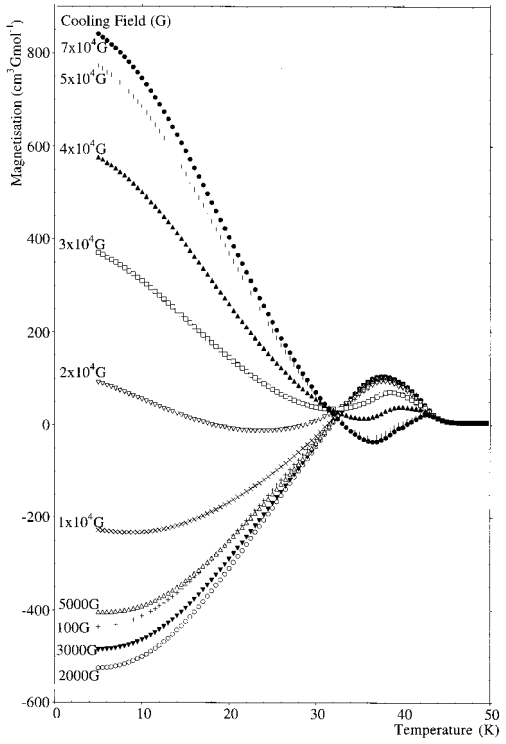

Figure 5. Temperature dependence of the FC (100−70 000 G) magnetization of $N(n\text{-}C_4H_9)_4Fe^{II}Fe^{III}(C_2O_4)_3$, on warming in 100 G.

displaced toward negative magnetization, indicating that the sample retains a memory of its field cooling history, despite field cycling between ±70 000 G. The fact that the hysteresis loop opens over the field cycle indicates that irreversible magnetization processes occur, although it shows no coercive field (H_c). The

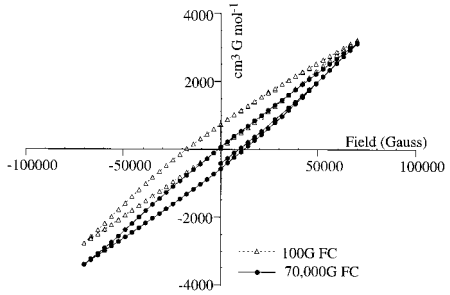

Figure 6. Hysteresis of $N(n\text{-}C_4H_9)_4Fe^{II}Fe^{III}(C_2O_4)_3$ at 5K after (a) 100-G FC and (b) 70 000-G FC.

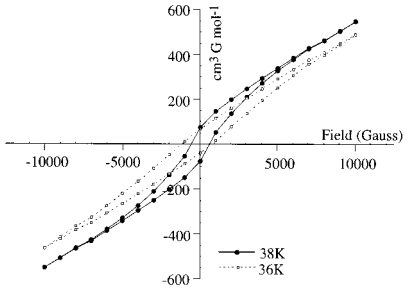

Figure 7. Variation of hysteresis of $N(n\text{-}C_4H_9)_4Fe^{II}Fe^{III}(C_2O_4)_3$ (100-G FC) with temperature.

Table 2. Temperature Dependence of the Coercivity (H_c) and Remanence (R_M) of $AFe^{II}Fe^{III}(C_2O_4)_3$

temp (K)	cooling field (G)	H_c (G)	R_M (cm³ G mol⁻¹) dec field	R_M (cm³ G mol⁻¹) inc field	$\lvert\Delta R_M\rvert$ (cm³ G mol⁻¹)
		(a) A = $(n\text{-}C_4H_9)_4$			
42	100	188	18	−22	40
40	100	400	60	−58	118
38	100	581	75	−75	150
36	100		69	−39	108
33	100		22	14	8
31	100		5	−13	18
29	100		−20	−64	44
5	100		58	−585	643
5	0		744	42	702
5	70000		330	−330	660
		(b) A = $P(C_6H_5)_4$			
25	100	0	0	0	40
20	100	541	140	−130	118
15	100	1200	280	−280	150
5	100	11500	890	−890	108

remanent magnetizations R_M are recorded in Table 2a for both increasing and decreasing applied fields. In contrast, the 70 000-G FC hysteresis curve at 5 K is asymmetrically displaced toward positive magnetization, indicating a memory effect in the opposite direction to the 100-G FC one, with respect to the cooling field, while the shape is almost identical to that after 100-G field cooling, with similar asymmetry and remanence values. Thus, the ground-state reached after cooling in 70 000 G is similar to the one arrived at cooling in 100 G, though with a reversal in the direction of the remanent magnetization.

The 100-G FC hysteresis loop opens below T_c and between 42 and 38 K retains a conventional *S*-shape, is symmetric with respect to the magnetization axis, and exhibits a coercive field (H_c). Such behavior is consistent with the growth of magnetic domains in the direction of applied field. Below 38 K, the hysteresis curve changes shape, becomes asymmetric, and has no observed coercivity ±10 000 G (Figure 7). On further cooling the hysteresis narrows and reduces its asymmetric shift until at 32 K (T_{comp}) it vanishes. Finally at 29 K it resembles the one recorded at 5 K. The temperature dependence of the magnetic coercivity and remanence constants are listed in Table 2a.

AC Susceptibility. Figure 8 shows the dispersion (χ') and the absorption (χ'') of the ac susceptibility at 0.1 Hz. Above T_c, χ' follows the dc susceptibility and $\chi'' = 0$, consistent with the measured quantity being the isothermal susceptibility, i.e., $\chi' = c_T = c_{dc}$ (wt ≪ 1). Below 47 K c' begins to rise, reaching a maximum at ∼44 K, in parallel with the onset of divergence between

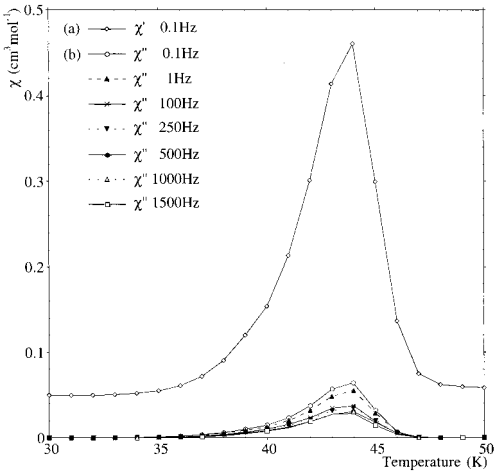

Figure 8. Ac susceptibilities of $N(n\text{-}C_4H_9)_4Fe^{II}Fe^{III}(C_2O_4)_3$ in ordering region: (a) χ' at 0.1 Hz; (b) frequency dependence of χ'' (0.1−1500 Hz).

the dc FC and ZFC susceptibilities. At lower temperature χ' falls, with a broad but weak shoulder at 40 K, analogous to that seen in the dc ZFC data. At 35 K χ' follows the ZFC χ_{dc}, consistent with the measured quantity now being the adiabatic susceptibility $\chi' = \chi_S$ (wt ≫ 1). Below 46 K χ'' rises from zero to a maximum at ∼44 K before falling to zero around 40 K. The nonzero χ'' between 40 and 46 K indicates that relaxational processes are active (wt ∼ 1) and confirms the transition to a state with a spontaneous magnetization. The maximum in χ'' at ∼44 K reduces in magnitude and broadens with increasing measurement frequency from 0.1 to 1500 Hz, though the temperature of the maximum remains constant (Figure 8).

Positive Low Temperature Magnetization. *Low Applied Field.* As an example of a compound showing positive low temperature magnetization, the magnetization of the $P(C_6H_5)_4$ salt was investigated under the same protocols as the $N(n\text{-}C_4H_9)_4$ compound. Both the ZFC and 100 G FC magnetizations rise at T_c ∼34 K but begin to diverge at 28 K. The ZFC magnetization reaches a broad maximum at around 25 K and then decreases toward lower temperatures reaching 6 cm³ G mol⁻¹ at 5 K (Figure 9). Magnetization curves measured after cooling in fields higher than 10 G have no maxima at 25 K. The saturation magnetization at 5 K increased monotonically with the cooling field, in each case with $\delta M/\delta T \rightarrow 0$.

High Field Studies. The high field hysteresis behavior of $P(C_6H_5)_4Fe^{II}Fe^{III}(C_2O_4)_3$ at 5 K (100-G FC) is plotted in Figure 10a, while the temperature evolution of hysteresis between ±10 000 G at 15, 20, and 25 K

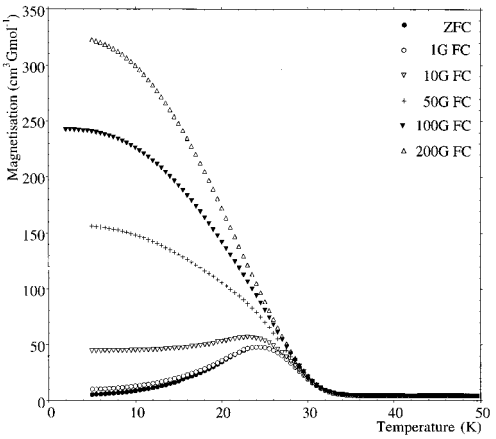

Figure 9. Temperature dependence of the ZFC and FC (1−200 G) magnetization of $P(C_6H_5)_4Fe^{II}Fe^{III}(C_2O_4)_3$.

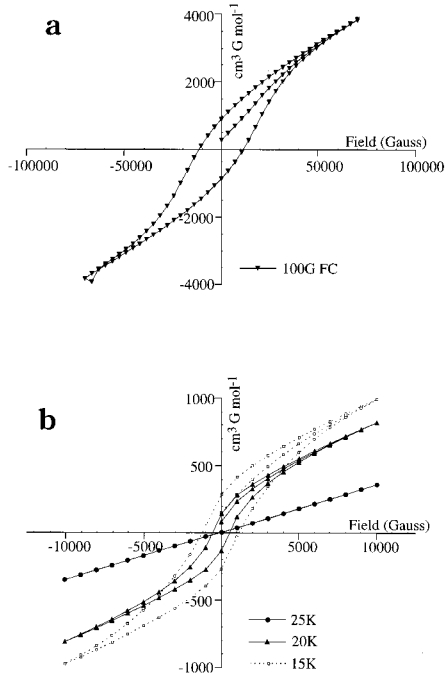

Figure 10. Hysteresis of $P(C_6H_5)_4Fe^{II}Fe^{III}(C_2O_4)_3$ (100-G FC): (a) 5K; (b) variation with temperature.

(100-G FC) is shown in Figure 10b. The hysteresis loop at 5 K is symmetric, indicating no field cooling memory, and has a coercive field (H_c) of 11 500 G. The temperature dependence of the hysteresis is unusual: at 25 K (corresponding to roughly the magnetization maximum in the ZFC data (Figure 9) and 9 K below T_c) there is no measurable opening of the hysteresis, but at lower temperatures it opens, resembling the 5 K curve (Figure 10b). The temperature-dependent magnetic coercivity and remanence constants are listed in Table 2b.

AC Susceptibility. Figure 11 shows the ac susceptibilities (χ' and χ'') measured at 0.1 Hz. At 45 K $\chi' \approx \chi_{dc} = \chi_T$ and the absorption $\chi'' = 0$ (wt $\ll$ 1). Upon lowering the temperature, χ' rises to a very small maximum at around 40 K and falls; χ' begins to rise gradually again at 35 K, with a shoulder near 30 K and a maximum ~18 K. At 5 K, χ' decreases to become equal to the ZFC dc magnetization. At its peak, χ' is considerably smaller than ZFC χ_{dc}. Furthermore, since χ' has no sharp peak it is not possible to estimate T_c from ac measurements.

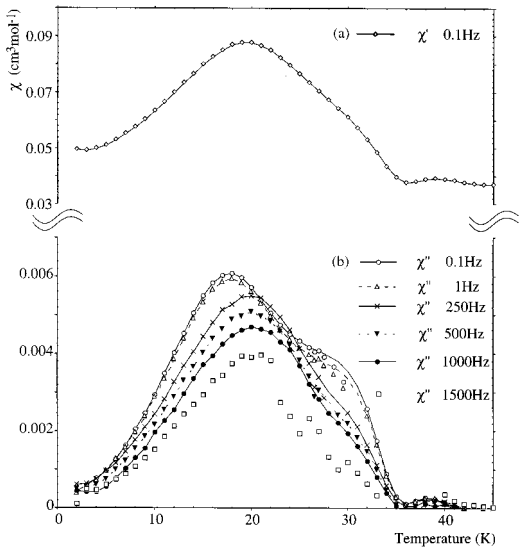

Figure 11. Ac susceptibilities of $P(C_6H_5)_4Fe^{II}Fe^{III}(C_2O_4)_3$ in ordering region: (a) χ' at 0.1 Hz; (b) frequency dependence of χ'' (0.1−1500 Hz).

The absorption, χ'', varies with temperature in the same way as χ' but with much smaller susceptibility. The behavior of both χ' and χ'' is extremely unusual and the fact that χ'' remains finite between 5 and 40 K indicates that at least some relaxation processes are active (wt ~ 1) down to low temperature. Figure 11b displays the frequency dependence of χ''. The maximum at 18 K becomes weaker and shifts to higher temperatures with increasing measuring frequency, the high temperature shoulder being present only at frequencies lower than 1 Hz. If we assume that there is a single time constant t for magnetic relaxation, the maximum in χ'' corresponds to a freezing temperature (T_f), below which the magnetization cannot follow the oscillating field. A test for Arrhenius magneto-dynamics indicated that the magneto-dynamics of this material are more complicated than that predicted by a single activation energy.

Discussion

Paramagnetic Region. As a background to looking in more detail at the unusual magnetic properties of the $AFe^{II}Fe^{III}(C_2O_4)_3$ compounds in their ordered state we first consider their behavior in the paramagnetic region. The susceptibilities of all members of the series obey the Curie−Weiss law from 150 to 300 K. The mean value of the Curie constant across the series (7.662 cm^3 mol^{-1} K) is consistent with the presence of high spin Fe^{III} and Fe^{II} ions: assuming spin-only moments $S(Fe^{III}) = {}^5/_2$ and $S(Fe^{II}) = 2$ and an isotropic Landé splitting factor, $g = 2$, for both ions calculates $C = 7.375$ cm^3 mol^{-1} K.

While it is a good approximation to the $^6A_{1g}$ ground state of the Fe^{III} ion, the assumption of a spin-only moment is a poor approximation for Fe^{II}. The ^5D ($L = 2$) free-ion state of $Fe^{II}(d^6)$ ions has orbital degeneracy and in a cubic ligand field the $^5T_{2g}$ ground term retains an orbital contribution to the total moment, so that the lowest spin−orbit state has $J = 1$. Introducing a trigonal distortion from the three bidentate oxalate ligands causes a further splitting of the $J = 1$ state so

that the resulting ground state is either a singlet ($M_J = 0$) or doublet ($M_J = \pm 1$).[9] The energy separation between the spin−orbit components in Fe^{II} is on the order of 200 cm^{-1}, so we expect an orbital contribution to the Fe^{II} moment, which could explain the high value of the Curie constant. The Curie constants of $N(n\text{-}C_3H_7)_4$, $N(n\text{-}C_4H_9)_4$, and $P(n\text{-}C_4H_9)_4$ compounds are all in excess of the spin-only value by approximately 0.43 cm^3 G mol^{-1}; however, for $N(n\text{-}C_5H_{11})_4Fe^{II}Fe^{III}(C_2O_4)_3$, $C = 9.05$ cm^3 G mol^{-1}, corresponding to an excess of approximately 1.6 cm^3 G mol^{-1} (Table 1). This might result from the different symmetry of the Fe^{II} sites: for $N(n\text{-}C_3H_7)_4$, $N(n\text{-}C_4H_9)_4$, and $P(n\text{-}C_4H_9)_4$ compounds the powder X-ray diffraction is modeled by a hexagonal cell with C_3 site symmetry of the $Fe^{II}(C_2O_4)_3$ unit,[6] while the site symmetry of Fe^{II} in the $N(n\text{-}C_5H_{11})_4$ compound is C_2.[5]

The Weiss constants θ are all large and negative, indicating a mean antiferromagnetic interaction between Fe moments. From the small spread in θ values (−86.9 to −92.2 K), we see that the magnetic exchange is of similar strength in all the compounds, as expected, given the close similarity between the structures. In most of the compounds $|T_c/\theta| \sim 0.5$, although for $P(C_6H_5)_4$ and $As(C_6H_5)_4$ it is ∼0.4. Molecular field theory predicts $|T_c/\theta| = 1$, but large deviations are expected in low dimensional magnets because of the buildup of short-range correlations above T_c. Indeed, for a two-dimensional Ising ferromagnet on a honeycomb lattice $|T_c/\theta|$ has been calculated as 0.506.[10] The reduced $|T_c/\theta|$ in the $P(C_6H_5)_4$ and $As(C_6H_5)_4$ compounds may therefore signal a change in the effective dimensionality.

Low-Temperature Magnetic Behavior. Below 100 K the magnetization of this series of compounds varies dramatically with the cation A. When measuring the magnetization after cooling in a 100 G field, a magnetic compensation point (T_{comp}) and low-temperature negative magnetization with respect to the field are observed in the A = $N(n\text{-}C_3H_7)_4$, $N(n\text{-}C_4H_9)_4$, $N(n\text{-}C_5H_{11})_4$, $P(n\text{-}C_4H_9)_4$, and PPN compounds, while the $P(C_6H_5)_4$ and $As(C_6H_5)_4$ compounds show a positive magnetization at low temperature. Since all the compounds are ferrimagnetic, with Fe^{III} and Fe^{II} ions ordered antiferromagnetically, it is useful to compare the temperature dependence of the magnetization with that predicted by Néel: the "normal" positive magnetization curves of the $P(C_6H_5)_4$ and $As(C_6H_5)_4$ compounds resemble the Néel type Q ferrimagnetic order, while the negative magnetization curves exhibit a variant of Néel type N order.

According to Néel, the ground state of a ferrimagnet is determined by the saturation magnetizations of each magnetic sublattice ($M_s(T = 0\ K)$) and their relative ordering rates with respect to temperature. A compensation temperature (T_{comp}) should occur in the magnetization if the sublattice with the smaller saturation magnetization initially orders more rapidly with decreasing temperature than the one with the larger saturation magnetization. In the honeycomb lattice

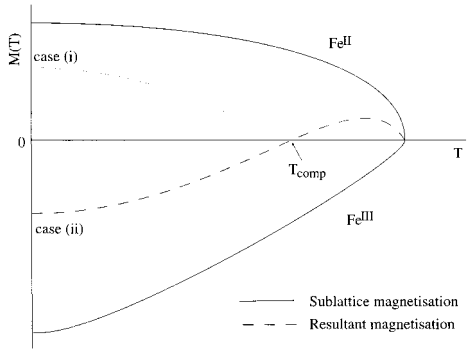

Figure 12. Magnetic sublattice ordering in a ferrimagnet containing Fe^{II} and Fe^{III} with Néel type N order.

with alternating Fe^{II} and Fe^{III} ions, this situation corresponds to an initially steeper ordering on the Fe^{II} sublattice, as shown schematically in Figure 12.

Evidence concerning the sublattice ordering in the $Fe^{II}Fe^{III}$ compounds comes from the Mössbauer spectra of the $N(n\text{-}C_4H_9)_4$ and $P(C_6H_5)_4$ compounds, from which the hyperfine field at the Fe^{III} nucleus has been extracted as a function of temperature for both compounds.[11] Within the molecular field approximation, the field experienced at the Fe^{III} nucleus is the sum of exchange fields which, to a first approximation, originate from the neighboring Fe^{II} ions. Hence, the development of a hyperfine field at the Fe^{III} nucleus provides a measure of the magnetization of the Fe^{II} sublattice and *vice versa*. The Mössbauer data indicate that there is a sharp increase in the Fe^{II} sublattice magnetization in the $N(n\text{-}C_4H_9)_4$ compound below 40 K. The temperature dependence of the Fe^{II} hyperfine field was not extracted from the data, although there was some indication that it was not fully developed ($H_{int} \sim 5$ T at 1.9 K). This provides evidence that the Fe^{II} sublattice does indeed order at a higher temperature than Fe^{III} in the $N(n\text{-}C_4H_9)_4$ compound. The situation in the $P(C_6H_5)_4$ case is more complex, with a hyperfine splitting at the Fe^{III} nucleus occurring only below 25 K.

The molecular field model predicts that the 0 K saturation magnetization of a two-sublattice ferrimagnet is the difference between the saturation magnetizations on each sublattice, which, in the magnetic order types N and Q, are both fully saturated. Therefore, in the hypothetical spin-only $Fe^{II}Fe^{III}$ case the saturation moment at 0 K would be $M_s(0\ K) = \pm g|S(Fe^{III}) - S(Fe^{II})|m_B = \pm 1 m_B$ (i.e., 1 spin per $Fe^{II}Fe^{III}$ unit) for type Q and type N ferrimagnetic order. In the negative magnetization compounds, we find saturation magnetization at 5 K (after 100-G FC) between −235 (PPN) and −850 cm^3 G mol^{-1} ($N(n\text{-}C_5H_{11})_4$), which corresponds to moments of between $0.0422 m_B$ and $0.1522 m_B$. In the compounds with positive magnetization the (100-G FC) saturation moment was $0.0435 m_B$ and $0.052 m_B$ for $P(C_6H_5)_4$ and $As(C_6H_5)_4$, respectively, much smaller than predicted by molecular field theory. However, in polycrystalline samples, crystallite orientations, noncrystallinity, and/or domain effects all contribute to reduce the saturation magnetization, though we note that in the $N(n\text{-}C_4H_9)_4$ compound a saturation moment of $\sim 0.07 m_B$ was reached at 5 K after cooling in fields between 2 and 5000 G.

(9) Figgis, B. N. *Introduction to Ligand Fields*; Interscience Publishers: New York, 1961.

(10) De Jongh, L. J. *Magnetic Properties of Layered Transition Metal Compounds*; Kluwer Academic Press: Dordrecht, 1990; Vol. 9.

(11) Ensling, J.; Nuttall, C. J.; Day, P., to be published.

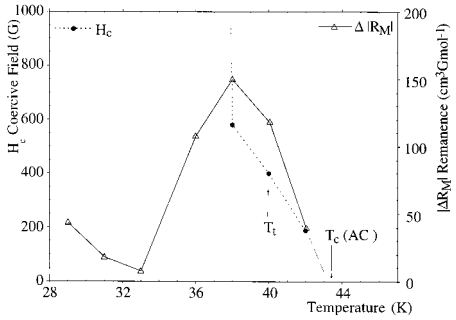

Figure 13. Temperature-dependent hysteresis parameters of $N(n\text{-}C_4H_9)_4Fe^{II}Fe^{III}(C_2O_4)_3$.

For a variety of reasons it is not appropriate to attempt a quantitative evaluation of the molecular field model to extract molecular field parameters. First, the honeycomb lattice is two-dimensional and therefore deviates considerably from the molecular field approximation as can be seen by the fact that $|T_c/\theta| = 0.5$. Furthermore, the Fe^{II} ion exhibits an orbital moment and hence its magnetization does not follow a Brillouin function. Finally, spin−orbit coupling in Fe^{II} introduces considerable anisotropy into the system that is not accounted for by the molecular field model.

Figure 12 illustrates two ways in which the magnetization in Néel type N ferrimagnets can vary with temperature. In case (i) the magnetization curve "bounces", as the magnetic pole reverses, i.e., $\{Fe^{II}(\uparrow)\text{-}Fe^{III}(\downarrow) \rightarrow Fe^{II}(\downarrow)Fe^{III}(\uparrow)\}$ at T_{comp}, resulting in positive magnetization at low temperature, while in case (ii) the initial magnetic pole direction is maintained and the magnetization becomes negative below T_{comp}. $N(n\text{-}C_4H_9)_4Fe^{II}Fe^{II}(C_2O_4)_3$ behaves like case (ii), although thermodynamically, positive magnetization is favored over negative at low temperature. In the molecular field approximation with fully isotropic exchange fields, there is no energy barrier to magnetic pole reversal, leading to magnetization similar to case (i). The fact that the $N(n\text{-}C_4H_9)_4$ salt conforms to case (ii) indicates that there is a barrier due to anisotropy sufficient to hinder pole reversal at T_{comp}.

The magnetic hysteresis loops of the $N(n\text{-}C_4H_9)_4$ compound reflect the anisotropy and stability of the negative magnetization, because a negative magnetization should be unstable to alignment with field above the anisotropy field H_a. However, the 5 K hysteresis of the $N(n\text{-}C_4H_9)_4$ compound shows no magnetic transition or coercive field (H_c) during field cycling between ±70 000 G but remains centered about the negative remanence, indicating a magnetic memory effect. The shape of the hysteresis and absence of a coercive field =70 000 G indicate that there is a giant anisotropy in the magnetization.

Parameters describing the temperature-dependent hysteresis in the $N(n\text{-}C_4H_9)_4$ compound are displayed in Figure 13, from which it is clear that the onset of giant anisotropy (H_c > 10 000 G) and the magnetic memory effect both occur between 36 and 38 K. Also the divergence in coercivity clearly correlates with narrowing of the hysteresis. In a ferrimagnet, the coercivity should diverge and the hysteresis narrow on approaching a compensation temperature[12] since $M_s(T = T_{comp}) = 0$. While the hysteresis loop in the $N(n\text{-}C_4H_9)_4$ salt is closed at T_{comp}, the pronounced change in magnetic characteristics between 36 and 38 K indicates that some form of magnetostrictive transition occurs between T_c and T_{comp}. Further evidence that there is such a transition comes from the low field measurements. The shoulder at 40 K in the ZFC magnetization is revealed as a discontinuity in the 100-G FC case. Indeed, we find similar discontinuities in the FC magnetization in all members of the series with negative magnetization at low temperature. However, it is important to note that it is the field cooling history through T_t and not T_c that is critical in determining the low-temperature negative magnetization: the negative magnetization is only reversed after cooling through T_c and T_t in fields = 60 000 G. The resulting positively magnetized state is identical to that obtained after 100-G FC, as indicated by the fact that the temperature dependence of magnetization is almost the inverse of the 100-G FC curve below T_t and that the hysteresis at 5 K is similar to the 100-G FC one, but asymmetrically displaced to positive magnetization.

Clearly the first-order discontinuity in the magnetization at T_t is the factor determining the low temperature magnetization properties of $AFe^{II}Fe^{III}(C_2O_4)_3$ compounds with negative magnetization. However, the physical origin of the transition has not been identified. One possibility is that at T_t the Fe^{II} moments lock due to an orbital ordering. If this is so, then cooling through T_t in small applied fields would provide the Fe^{II} moments with a preferred ordering direction. Provided the ferrimagnetic order conforms to the Néel type N, the magnetization will then become negative at low temperatures. The anisotropy developing below T_c due to a magnetostrictive orbital ordering of the Fe^{II} moments would be very large, as observed. A structural phase transition should also occur at T_t as the Fe^{II} moments couple to the lattice, but to date there are no low temperature structural data on any of these compounds. Nevertheless, the discontinuity in the magnetization points strongly to such a phase transition. Orbital ordering transitions occur when unquenched orbital moments align cooperatively below a magnetic ordering transition as a consequence of the spin−orbit coupling interaction. The theory developed by Goodenough[13] has been used to explain the negative magnetization and anisotropy behavior in the ferrimagnetic spinel[14] $Co[CoV]O_4$[14] and in the antiferromagnet $LaVO_3$.[15,16]

Returning to the magnetization behavior in $P(C_6H_5)_4$ and $As(C_6H_5)_4$ compounds, which correspond to Néel type Q ferrimagnetic order, one question remaining is why there is such a large difference between the magnetic behavior in these compounds and those behaving like Néel type N. It is therefore pertinent to examine the behavior of the $P(C_6H_5)_4$ compound more closely and contrast it with the $N(n\text{-}C_4H_9)_4$ case. First, the transition to long-range magnetic order is less

(12) Standley, K. J. *Oxide Magnetic Materials*; Clarendon Press: Oxford, 1962.

(13) Goodenough, J. B. *Phys. Rev.* **1968**, *171*, 466−479.
(14) Menyuk, N.; Dwight, K.; Wickam, D. G. *Phys. Rev. Lett.* **1996**, *4*, 119−120.
(15) Goodenough, J. B.; Nguyen, H. C. *C. R. Acad. Sci. Paris* **1994**, *319* (*II*), 1285−1291.
(16) Nguyen, H.; Goodenough, J. B. *Phys. Rev. B* **1995**, *52*, 325−335.

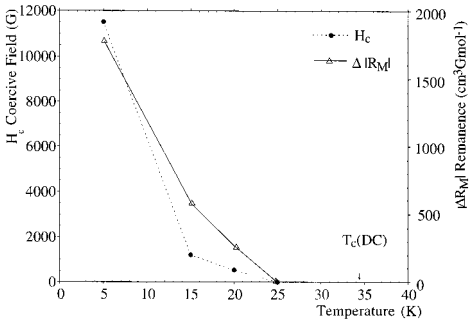

Figure 14. Temperature-dependent hysteresis parameters of $P(C_6H_5)_4Fe^{II}Fe^{III}(C_2O_4)_3$.

abrupt than in the $N(n\text{-}C_4H_9)_4$ compound. The increase in dc magnetization occurs at 34 K, which we assign as T_c. However, the ac susceptibility shows no sharp peak, either in dispersion or absorption. Furthermore, the ac susceptibility is strongly frequency dependent, while hysteresis is only observed below 25 K. This behavior contrasts with the $N(n\text{-}C_4H_9)_4$ case where ac susceptibility, Mössbauer, and hysteresis measurements all indicate a sharp magnetic transition between 43.5 and 40 K. The temperature dependence of the hysteresis parameters of the $P(C_6H_5)_4$ salt (Figure 14) are quite different from those of the $N(n\text{-}C_4H_9)_4$ one (Figure 13).

Neutron powder diffraction of $P(C_6D_5)_4Fe^{II}Fe^{III}(C_2O_4)_3$ reveals only weak asymmetric magnetic scattering intensity below 38 K at the [201] reciprocal lattice point, attributed to moments ordering parallel to the *c*-axis.[17] Although coherent magnetic scattering is evidence of long-range magnetic order, the weak scattering in $P(C_6D_5)_4Fe^{II}Fe^{III}(C_2O_4)_3$, in comparison to $P(C_6D_5)_4Mn^{II}\text{-}Fe^{III}(C_2O_4)_3$, indicates that long-range magnetic order is not completely developed in the former, even at 5 K, either as a result of a finite spin correlation length or because only part of the sample undergoes a transition to long-range magnetic order. From these diverse strands of evidence the most consitent view of the magnetic order in $P(C_6H_5)_4Fe^{II}Fe^{III}(C_2O_4)_3$ is that it is glassy. Below 34 K, ferrimagnetic correlations begin to develop with randomly oriented anisotropy, so that at 22−25 K the correlated regions become blocked by one another and hysteresis develops. Below the blocking temperature the bulk of the moments are fixed by anisotropy pinning, while a fraction remains mobile down to 5 K. The reasons for such glassy magnetic ordering could lie in a small deficiency of Fe and the charge compensating oxidation process $Fe^{II} \rightarrow Fe^{III}$, which introduces disorder in the magnetic sublattices. Such disorder would produce random anisotropies among the Fe^{II} moments. Hence, ferrimagnetically correlated regions of random anisotropy may develop, pinned to the Fe^{II} moments. When the correlated regions of different anisotropy interact, magnetic frustration and consequent glassy ordering would occur.

(17) Nuttall, C. J.; Day, P. *Inorg. Chem.*, in press.

Conclusions

We have undertaken a comprehensive study of the temperature dependent magnetization of two members of the series of layer molecular based ferrimagnets $AFe^{II}Fe^{III}(C_2O_4)_3$ ($A = N(n\text{-}C_4H_9)_4$ and $P(C_6H_5)_4$) in a range of zero field and applied field protocols. Our aim has been to map and then identify the reason for the appearance of negative magnetization at low temperature in the $N(n\text{-}C_4H_9)_4$ salt but not in the $P(C_6H_5)_4$ one. The two types of behavior correspond to Néel's type N and Q categories of ferrimagnetism. The negative magnetization becomes established above very low cooling fields (2 G) and increases in magnitude until around 2000 G. It is progressively reversed with higher cooling fields and becomes completely reversed above 60 000 G. As a result of the field cooling, the magnetization remanence at 5 K displays an asymmetric hysteresis with a giant anisotropy. The onset of giant anisotropy is identified with the presence of a discontinuity in the magnetization at $T_t = 40$ K ($T_{comp} < T_t < T_c$), which is assigned to a magnetostrictive transition, accompanied by alignment of the Fe^{II} local anisotropy axes. It is this transition, in low cooling fields, that is responsible for the stability of the negative magnetization. By contrast, in the $P(C_6H_5)_4$ compound, where no such discontinuity is found, full long-range magnetic order is not achieved, but a proportion of the moments remain mobile well below T_c. We ascribe this to the buildup of domains of correlated moments with randomly oriented anisotropy axes, which become fixed below a blocking temperature. More detailed crystallographic studies at low temperature will be needed to answer the final key question as to why the substitution of one organic cation by another should trigger such a profound change in the magnetic order in these otherwise very similar lattices.

Acknowledgment. We thank Dr. Simon Carling for help with the SQUID measurements at the RI and Professor K. Yakushi and Dr. Y. Nakazawa of the Institute of Molecular Sciences, Okazaki, Japan, for assisting with the AC susceptibility work. The project is supported by the U.K. Engineering and Physical Sciences Research Council. C.J.N. is also grateful for a MONBUSHO fellowship, awarded through the auspices of the British Council.

CM980177G